

Density-wave theory of dislocations in crystals

M. Raj Lakshmi, H. R. Krishna-Murthy, and T. V. Ramakrishnan
Department of Physics, Indian Institute of Science, Bangalore 560012, India

(Received 19 May 1987)

The density-wave theory of Ramakrishnan and Yussouff is extended to provide a scheme for describing dislocations and other topological defects in crystals. Quantitative calculations are presented for the order-parameter profiles, the atomic configuration, and the free energy of a screw dislocation with Burgers vector $\mathbf{b}=(a/2, a/2, a/2)$ in a bcc solid. These calculations are done using a simple parametrization of the direct correlation function and a gradient expansion. It is conventional to express the free energy of the dislocation in a crystal of size R as $(\lambda b^2/4\pi)\ln(\alpha R/|b|)$, where λ is the shear elastic constant, and α is a measure of the core energy. Our results yield for Na the value $\alpha \approx 1.94a/(|c_1''|)^{1/2} (\approx 1.85)$ at the freezing temperature (371 K) and $\alpha \approx 2.48a/(|c_1''|)^{1/2}$ at 271 K, where c_1' is the curvature of the first peak of the direct correlation function $c(q)$. Detailed results for the density distribution in the dislocation, particularly the core region, are also presented. These show that the dislocation core has a columnar character. To our knowledge, this study represents the first calculation of dislocation structure, including the core, within the framework of an order-parameter theory and incorporating thermal effects.

I. INTRODUCTION

In this paper, we present a new approach for describing dislocations and other topological defects in crystals. This approach is an extension of the density-wave theory of Ramakrishnan and Yussouff¹⁻³ to allow for topological singularities in the phase of the density wave.

Earlier approaches used for studying dislocations and other defects have employed either the continuum elastic approximation⁴ or atomic models.⁵⁻⁷ Both these approaches have several drawbacks. The continuum elasticity theory fails where the deformation is large, e.g., for dislocation cores. The atomic model is too detailed and requires poorly known interatomic potentials. It is known that some of the core properties are highly sensitive to the assumed interatomic potentials. Also, it is basically a zero-temperature theory and is not easily extended to nonzero temperatures. Neither approach makes connection with the fact that much of strong de-

formation behavior depends only on structure.

In contrast, our approach is structural and has the following advantages over the earlier two schemes:

(i) Our scheme reduces to the correct elastic continuum theory far away from the core of the dislocation with the elastic constants as given by the density-wave theory.^{3,8} But the core region is adequately handled, unlike in the continuum elasticity approach.

(ii) Thermal, statistical-mechanical effects are included from the outset, in contrast to the atomistic description.

(iii) The parameters (the direct correlation function, etc.) which are inputs to the theory are structural properties of the (supercooled) liquid which are either directly measurable or can be related to measured quantities.

Below we summarize the essential features of our approach and our major results.

In the density-wave theory of freezing,¹ the following functional gives the excess free energy for creating a general density profile $\rho(\mathbf{r})$ in a liquid of uniform density ρ_l :

$$\frac{\Omega - \Omega_l}{k_B T} = \beta \int d\mathbf{r} U_e(\mathbf{r})[\rho(\mathbf{r}) - \rho_l] + \int d\mathbf{r} \rho(\mathbf{r}) \ln[\rho(\mathbf{r})/\rho_l] - \int d\mathbf{r} [\rho(\mathbf{r}) - \rho_l] - \frac{1}{2} \int d\mathbf{r} \int d\mathbf{r}_1 c^{(2)}(\mathbf{r} - \mathbf{r}_1) [\rho(\mathbf{r}) - \rho_l][\rho(\mathbf{r}_1) - \rho_l] + \dots, \tag{1.1}$$

where $U_e(\mathbf{r})$ is the external potential and $c^{(2)}(\mathbf{r})$ is the direct correlation function of the (supercooled) liquid. Minimization of Ω gives the self-consistent equation

$$\rho(\mathbf{r}) = \rho_l \exp \left\{ -\beta U_e(\mathbf{r}) + \int d\mathbf{r}_1 c^{(2)}(\mathbf{r} - \mathbf{r}_1) \times [\rho(\mathbf{r}_1) - \rho_l] + \dots \right\}, \tag{1.2}$$

the lowest-free-energy solution of which is the stable configuration.

Specifically one finds that,¹ if $c^{(2)}$ is large enough, then the self-consistent equation (1.2) supports solutions with crystalline periodicity and symmetry of the form

$$\rho(\mathbf{r}) = \rho_l \left[1 + \sum_{\mathbf{G}} \mu_{\mathbf{G}} e^{i\mathbf{G} \cdot \mathbf{r}} \right],$$

where $\{\mathbf{G}\}$ is the set of reciprocal-lattice vectors. If,

furthermore, the free energy corresponding to such a solution is lower than that of the liquid, then the crystal is the stable state of the system.

We represent crystals with defects in terms of inhomogeneous density-wave states of the form

$$\rho(\mathbf{r}) = \rho_l \left[1 + \sum_{\mathbf{G}} \eta_{\mathbf{G}}(\mathbf{r}) e^{i\mathbf{G}\cdot\mathbf{r}} \right], \quad (1.3)$$

where, in general, $\eta_{\mathbf{G}}(\mathbf{r})$ are complex:

$$\{\eta_{\mathbf{G}}(\mathbf{r})\} = \{\mu_{\mathbf{G}}(\mathbf{r}) e^{i\phi_{\mathbf{G}}(\mathbf{r})}\}.$$

In particular, dislocations are topological defects and are characterized by the fact that in going around its core, the phases of the order parameters change by integral multiples of 2π , i.e., $\oint d\phi_{\mathbf{G}} = 2n_{\mathbf{G}}\pi$. For example, in the case of a crystal with a screw dislocation along the z axis, we can write

$$\rho(\mathbf{r}) = \rho_l \left[1 + \eta_0(\mathbf{r}) + \sum_{\mathbf{G}(\neq 0)} \mu_{\mathbf{G}}(\mathbf{r}) \times \exp(i\mathbf{G}\cdot\hat{\mathbf{z}}b\phi/2\pi) e^{i\mathbf{G}\cdot\mathbf{r}} \right], \quad (1.4)$$

where $b\hat{\mathbf{z}}$ is the Burgers vector of the dislocation and $\eta_0(\mathbf{r}), \mu_{\mathbf{G}}(\mathbf{r})$ tend to $\eta_0^*, \mu_{\mathbf{G}}^*$, the crystalline solid values,

$$\mathbf{G} = \{(2\pi/a)(1, 1, 0), (2\pi/a)(-1, -1, 0), (2\pi/a)(0, 1, 1), (2\pi/a)(0, -1, -1), (2\pi/a)(1, 0, 1), (2\pi/a)(-1, 0, -1)\}$$

for which $\phi_{\mathbf{G}} \neq 0$, and $\xi_{\mathbf{G}} = \xi_2$ for the other six vectors

$$\mathbf{G} = \{(2\pi/a)(1, -1, 0), (2\pi/a)(-1, 1, 0), (2\pi/a)(0, 1, -1), (2\pi/a)(0, -1, 1), (2\pi/a)(1, 0, -1), (2\pi/a)(-1, 0, 1)\}$$

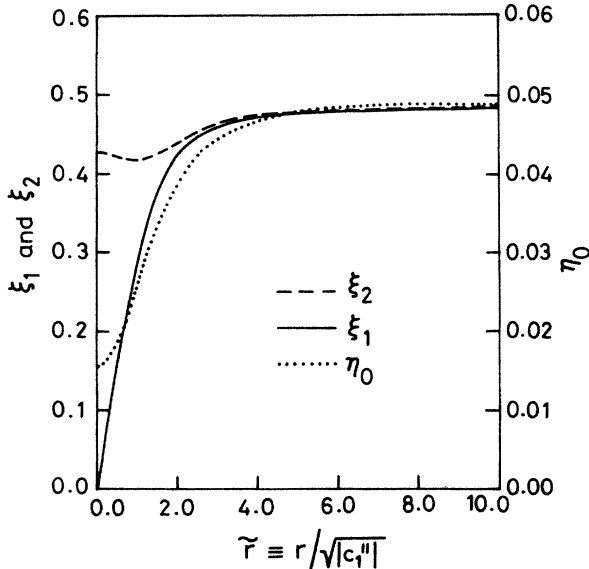


FIG. 1. Profiles of the molecular-field components $\xi_1(r)$ and $\xi_2(r)$, and the fractional density change $\eta_0(r)$ for a $\frac{1}{2}a(1,1,1)$ screw dislocation in a bcc solid at freezing (sodium at $T = T_m = 371$ K). $\tilde{r} = r/|c_1''|^{1/2}$ is the reduced radial distance from the dislocation axis.

as $(x^2 + y^2) \rightarrow \infty$.

Under the assumption that $\{\eta_{\mathbf{G}}(\mathbf{r})\}$ vary slowly on the scale of the unit cell and of the range of $c^{(2)}(\mathbf{r})$, one can make^{2,9} a gradient expansion plus a local approximation of the free-energy functional (1.1). Minimizing this approximate functional with respect to $\eta_{\mathbf{G}}(\mathbf{r})$, one gets differential equations for $\eta_{\mathbf{G}}(\mathbf{r})$, which are to be solved numerically subject to the appropriate boundary conditions (see Sec. IV).

In this paper we show that the numerical computations are very much simplified if we work with $\{\xi_{\mathbf{G}}(\mathbf{r})\}$, the Fourier components of the molecular field $\xi(\mathbf{r}) = \ln[\rho(\mathbf{r})/\rho_l]$, rather than with $\{\eta_{\mathbf{G}}(\mathbf{r})\}$.

The specific dislocation we discuss in detail in this paper, is the $\frac{1}{2}a(1,1,1)$ screw dislocation in a bcc crystal as it presents the simplest problem computationally. To further simplify the numerics, we do not keep all of $c^{(2)}(q)$, the Fourier transform of $c^{(2)}(r)$, but take only c_0, c_1 , and c_1'' to be nonzero, where c_0 and c_1 are the values of $c^{(2)}(q)$ at $q=0$ and at its first peak, respectively, and c_1'' is the second derivative of $c^{(2)}(q)$ at its first peak. In this approximation, $\{\xi_{\mathbf{G}}\}$ are nonzero only for $\mathbf{G}=0$ and for the first set of reciprocal-lattice vectors $\{\mathbf{G}\} = \{(2\pi/a)(1,1,0)\}$. ξ_0 determines the fractional mean density change η_0 via the relation $\eta_0 \equiv \xi_0/c_0$. By the symmetry of the problem, only two amplitudes $\xi_1(r)$ and $\xi_2(r)$ are sufficient to characterize $\{\xi_{\mathbf{G}}\}$; $\xi_{\mathbf{G}} = \xi_1$ for the six vectors

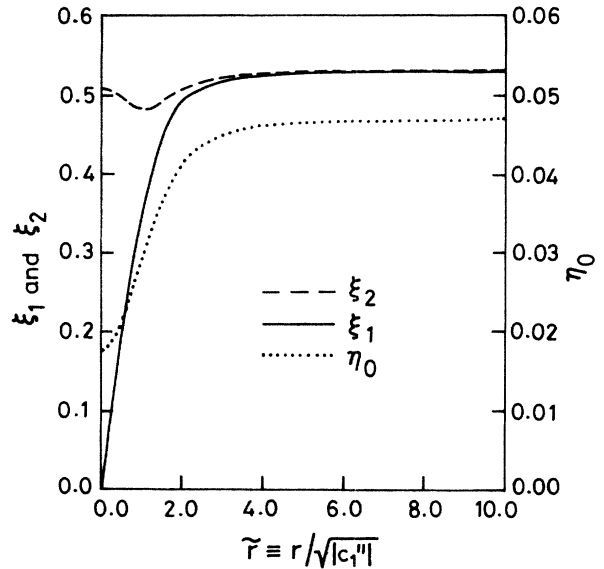


FIG. 2. Profiles of the molecular-field components $\xi_1(r)$ and $\xi_2(r)$, and the fractional density change $\eta_0(r)$ for a $\frac{1}{2}a(1,1,1)$ screw dislocation in a bcc solid below freezing (sodium at $T = T_m - 100$ K = 271 K). $\tilde{r} = r/|c_1''|^{1/2}$ is the reduced radial distance from the dislocation axis.

for which $\phi_G = 0$. Furthermore, all these amplitudes are functions only $\bar{r} = [r / (|c_1''|)^{1/2}]$, where r is the radial distance from the axis of the dislocation.

Our results for the order-parameter profiles $\xi_1(\bar{r})$, $\xi_2(\bar{r})$, and $\eta_0(\bar{r})$ are shown in Fig. 1 for $T = T_m$ (the freezing temperature), and in Fig. 2 for $T = T_m - 100$ K, for sodium. The input parameters have been obtained from extrapolations of experimental data. These figures show that the radii of the cores are approximately 2–3 lattice spacings. Note that $\xi_1(r)$, which characterizes $\xi_G(r)$ for those G for which $\phi_G \neq 0$, vanishes at the core of the dislocation.

Using the order-parameter profiles, we can calculate the (free) energy of the dislocation. Expressing the re-

sults in the conventional form⁴ $(\lambda b^2/4\pi)\ln(\alpha R/b)$, where λ is the shear elastic constant, and R the radial size of the sample, we get for α , which is a measure of the core energy, the following values:

$$(i) \text{ at } T = T_m, \alpha = 1.94a / (|c_1''|)^{1/2} \simeq 1.85;$$

$$(ii) \text{ at } T = T_m - 100 \text{ K}, \alpha = 2.48a / (|c_1''|)^{1/2}.$$

By way of comparison, the only other calculation of the core energy, the zero-temperature atomistic description, gives⁵⁻⁷ $\alpha \sim 4-5$.

Within our formulation, we can also calculate the atomic configuration of the dislocation. The density profile in the solid with the screw dislocation is given by

$$\begin{aligned} \rho_D(\mathbf{r}) &= \rho_l \exp[\xi_D(\mathbf{r})], \\ \xi_D(\mathbf{r}) &= c_0 \eta_0 [(x^2 + y^2)^{1/2} a |c_1''|^{-1/2}] \\ &+ 2\xi_1 [(x^2 + y^2)^{1/2} a |c_1''|^{-1/2}] \left\{ \cos \left[2\pi \left[\sqrt{2/3}y + \frac{2}{\sqrt{3}}z + \phi/2\pi \right] \right] \right. \\ &\quad \left. + 2 \cos \left[2\pi \left[\frac{1}{\sqrt{2}}x - \frac{1}{3} \right] \right] \cos \left[2\pi \left[-\frac{1}{\sqrt{6}}y + \frac{2}{\sqrt{3}}z + \phi/2\pi \right] \right] \right\} \\ &+ 2\xi_2 [(x^2 + y^2)^{1/2} a |c_1''|^{-1/2}] \left\{ \cos[2\pi(\sqrt{2}x - \frac{2}{3})] + 2 \cos \left[2\pi \left[\frac{1}{\sqrt{2}}x - \frac{1}{3} \right] \right] \cos[2\pi(\sqrt{3}/2y)] \right\}, \end{aligned} \quad (1.5)$$

where x, y, z are in units of a , and ϕ is the azimuthal angle about the z axis which is the axis of the dislocation. The origin for x and y has been chosen to be at the center of a triangle in the triangular lattice obtained by projection of the bcc lattice on to its (111) plane. Using the order-parameter profiles given in Fig. 1, we can locate the positions of the maxima of $\rho_D(\mathbf{r})$. We find that if these are identified with the atomic positions in the presence of the dislocation, the results are very close to what would be obtained using the continuum elasticity description,^{5,7} *even inside the core region*. That is, these maxima are displaced relative to the maxima in the uniform solid mainly along the z axis, by an amount $\mathbf{u} = (\mathbf{b}/2\pi)\tan^{-1}(y/x)$; the displacements normal to z are very small.

However, an examination of the actual density distribution $\rho_D(\mathbf{r})$ in the presence of the dislocation shows that the core region is greatly modified compared to the uniform solid. Because $\xi_1(r)$ vanishes at the axis of the dislocation, the modulation of $\rho_D(\mathbf{r})$ parallel to the z axis is very small within the core. Thus the dislocation core has a columnar character. We believe that ours is the first calculation to reveal this picture of the core region. The details are presented in Sec. VI. Note that $\rho_D(\mathbf{r})$ is periodic in the z direction with the same periodicity as the uniform crystal.

The rest of this paper is organized as follows: In order to make this paper self-contained, we recapitulate the essentials of the density-wave theory and its application to inhomogeneous solids in general in Sec. II. In Sec. III we present our scheme for treating dislocations

in crystals. This scheme is applied to the $\frac{1}{2}a(1,1,1)$ screw dislocation in the bcc solid in Sec. IV. The calculational details are given in Sec. V, where we also introduce the molecular field and show its usefulness. In Sec. VI, we discuss the results of our calculations. We discuss the limitations of our present study, possible further improvements, and other applications of the theory in Sec. VII.

II. THE RAMAKRISHNAN-YUSSOUFF THEORY OF FREEZING

The basic philosophy of the Ramakrishnan-Yussouff theory of freezing is that the solid is regarded as a calculable perturbation on the liquid, and various of its properties are obtained in terms of the fluid-phase correlations.

In an ideal fluid, an externally applied potential $U_e(\mathbf{r})$ induces a spatially varying local density according to Boltzman's law:

$$\rho(\mathbf{r}) = \rho_{id} \exp[-\beta U_e(\mathbf{r})]$$

where

$$\rho_{id} = (2\pi m / \beta h^2)^{3/2} \exp(\beta \mu).$$

In a nonideal fluid, because of the presence of interactions, within a mean-field description the external potential is augmented by an induced internal potential, or molecular field, which we denote $[-\xi(\mathbf{r})/\beta]$. In this case the local density is

$$\rho(\mathbf{r}) = \rho_{\text{id}} \exp[-\beta U_e(\mathbf{r}) + \xi(\mathbf{r})].$$

In general, $\xi(\mathbf{r})$ is a functional of $U_e(\mathbf{r})$, or equivalently of $\rho(\mathbf{r})$. Consider expanding $\xi(\mathbf{r})$ as a functional Taylor

$$\rho(\mathbf{r}) = \rho_l \exp \left[-\beta U_e(\mathbf{r}) + \int d\mathbf{r}_1 c^{(2)}(\mathbf{r}, \mathbf{r}_1) [\rho(\mathbf{r}_1) - \rho_l] + \frac{1}{2} \int d\mathbf{r}_1 \int d\mathbf{r}_2 c^{(3)}(\mathbf{r}, \mathbf{r}_1, \mathbf{r}_2) [\rho(\mathbf{r}_1) - \rho_l] [\rho(\mathbf{r}_2) - \rho_l] + \cdots \right]. \quad (2.1)$$

Here the zeroth-order molecular field converts ρ_{id} into ρ_l . By considering the perturbative response of $\rho(\mathbf{r})$ to a small external potential, it is easy to show that $c^{(2)}(\mathbf{r}, \mathbf{r}_1)$ and $c^{(3)}(\mathbf{r}, \mathbf{r}_1, \mathbf{r}_2)$ are to be interpreted as the *measured* second- and third-order direct correlation functions in the liquid state. In particular $\rho_l c_k^{(2)} = (1 - S_k^{-1})$, where S_k is the static structure factor of the liquid, and

$$\rho_l c_0^{(2)} = (1 - S_0^{-1}) = (1 - \beta / \rho_l \kappa_T),$$

where κ_T is the compressibility of the liquid.

The self-consistent equation for $\rho(\mathbf{r})$, Eq. (2.1), can also be thought of as arising from the minimization of the following free-energy functional:

$$\begin{aligned} \beta(\Omega - \Omega_l) = & \beta \int d\mathbf{r} U_e(\mathbf{r}) [\rho(\mathbf{r}) - \rho_l] + \int d\mathbf{r} \rho(\mathbf{r}) \ln[\rho(\mathbf{r}) / \rho_l] - \int d\mathbf{r} [\rho(\mathbf{r}) - \rho_l] \\ & - \frac{1}{2} \int d\mathbf{r} \int d\mathbf{r}_1 c^{(2)}(\mathbf{r}, \mathbf{r}_1) [\rho(\mathbf{r}) - \rho_l] [\rho(\mathbf{r}_1) - \rho_l] \\ & - \frac{1}{3!} \int d\mathbf{r} \int d\mathbf{r}_1 \int d\mathbf{r}_2 c^{(3)}(\mathbf{r}, \mathbf{r}_1, \mathbf{r}_2) [\rho(\mathbf{r}) - \rho_l] [\rho(\mathbf{r}_1) - \rho_l] [\rho(\mathbf{r}_2) - \rho_l] + \cdots, \end{aligned} \quad (2.2)$$

where Ω_l is the free energy of the uniform liquid. Here, the first two terms are essentially the ideal-gas term (except for the replacement of ρ_{id} by ρ_l). The remaining part of the free energy has again been expanded as a functional Taylor series in $[\rho(\mathbf{r}) - \rho_l]$. (The first-order term converts ρ_{id} to ρ_l .)

The whole point is that, even when $U_e = 0$, Eq. (2.1) can support solutions other than $\rho = \rho_l$ if $c^{(2)}$ and $c^{(3)}$ are sufficiently large. In particular, consider three-dimensional (3D) density-wave states of crystalline periodicity and symmetry:

$$\rho(\mathbf{r}) = \rho_l \left[1 + \sum_{\mathbf{G}} \eta_{\mathbf{G}} e^{i\mathbf{G} \cdot \mathbf{r}} \right], \quad (2.3)$$

where $\{\mathbf{G}\}$ is the set of reciprocal-lattice vectors. η_0 is the fractional density change, and $\{\eta_{\mathbf{G}} (\mathbf{G} \neq 0)\}$ are the Fourier components of the periodic density. The self-consistent equation (2.1) now reduces to

$$1 + \sum_{\mathbf{G}} \eta_{\mathbf{G}} e^{i\mathbf{G} \cdot \mathbf{r}} = \exp \left[\sum_{\mathbf{G}} c_{\mathbf{G}} \eta_{\mathbf{G}} e^{i\mathbf{G} \cdot \mathbf{r}} \right], \quad (2.4)$$

where we have ignored $c^{(3)}$ (and all higher-order correlation functions) for simplicity (*as we shall do for the rest of this paper*), and denoted $\rho_l c_{\mathbf{G}}^{(2)} \equiv c_{\mathbf{G}}$. The free-energy functional is

$$\begin{aligned} \frac{\beta(\Omega - \Omega_l)}{\rho_l V} = & \frac{1}{v} \int^{\text{cell}} d\mathbf{r} \left[1 + \sum_{\mathbf{G}} \eta_{\mathbf{G}} e^{i\mathbf{G} \cdot \mathbf{r}} \right] \\ & \times \ln \left[1 + \sum_{\mathbf{G}} \eta_{\mathbf{G}} e^{i\mathbf{G} \cdot \mathbf{r}} \right] \\ & - \eta_0 - \frac{1}{2} \sum_{\mathbf{G}} c_{\mathbf{G}} |\eta_{\mathbf{G}}|^2. \end{aligned} \quad (2.5)$$

Minimization with respect to $\eta_{\mathbf{G}}$ yields a set of equations which is equivalent to Eq. (2.4). If $\{c_{\mathbf{G}}\}$ are large enough, (2.4) has solutions with nonzero values for $\eta_{\mathbf{G}}$, which we will denote by $\eta_{\mathbf{G}}^*$. The minimized free energy, for $\eta_{\mathbf{G}} = \eta_{\mathbf{G}}^*$, is given by

$$\frac{\beta(\Omega_s - \Omega_l)}{\rho_l V} = (c_0 - 1) \eta_0^* + \frac{1}{2} \sum_{\mathbf{G}} c_{\mathbf{G}} |\eta_{\mathbf{G}}^*|^2. \quad (2.6)$$

(In principle one has to further minimize Ω_s with respect to the choice of $\{\mathbf{G}\}$.) If $\Omega_s > \Omega_l$, this crystalline state is metastable. As the temperature is reduced,

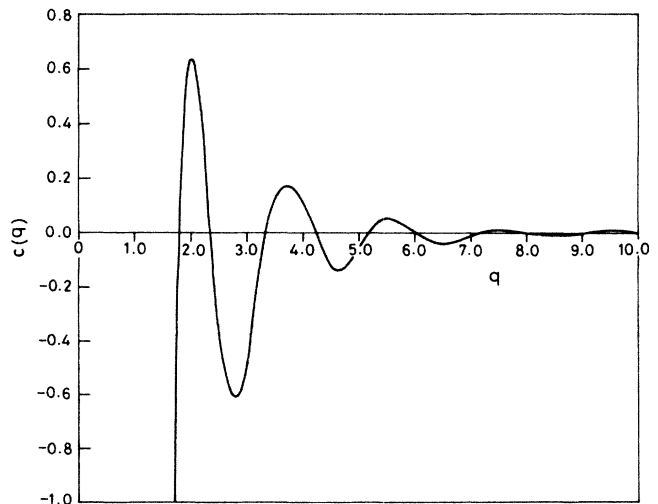


FIG. 3. The direct correlation function $c(q)$ for sodium at $T = 378$ K ($= T_f + 6$ K).

typically $\{c_G\}$ increase, and Ω_s decreases, until eventually $\Omega_s \leq \Omega_l$, whence the crystal becomes the stable phase, and the liquid freezes when $\Omega_s = \Omega_l$.

A typical $c(q)$ -versus- q curve is shown in Fig. 3. Certainly $c(q)$ decreases rapidly for large q . Suppose one sets $c_G = 0$ for all but $G=0$ and the first n sets of reciprocal-lattice vectors $\{\mathbf{G}_i^{(s)}\}$, $s=1, 2, \dots, n$. Here $\{\mathbf{G}_i^{(s)}\}$ for a given set s are z_s reciprocal-lattice vectors related by the point-group symmetry operations of the crystal, and will, hence, all have the same $c_{\mathbf{G}_i^{(s)}} \equiv c_s$ as well as the same $\eta_{\mathbf{G}_i^{(s)}}^* \equiv \eta_s^*$. It is easy to obtain the following $(n+1)$ coupled equations that determine $\{\eta_s^*\}$, $s=0, 1, \dots, n$, from (2.4):

$$\begin{pmatrix} 1 + \eta_0^* \\ \eta_s^* \end{pmatrix} = e^{c_0 \eta_0^*} \frac{1}{v} \int^{\text{cell}} d\mathbf{r} \begin{pmatrix} 1 \\ w_s(\mathbf{r}) \end{pmatrix} \exp \left[\sum_{s=1}^n c_s \eta_s^* z_s w_s(\mathbf{r}) \right]. \quad (2.7)$$

Here $w_s(\mathbf{r}) = (1/z_s) \sum_{i=1}^{z_s} \exp(i\mathbf{G}_i^{(s)} \cdot \mathbf{r})$, and v is the volume of a unit cell of the lattice. The remaining $\{\eta_G^*\}$ (for those G for which c_G has been set to zero) are determined in terms of the above $\{\eta_s^*\}$ simply by the integrals:

$$\eta_G^* = \exp(c_0 \eta_0^*) \frac{1}{v} \int^{\text{cell}} d\mathbf{r} e^{-i\mathbf{G} \cdot \mathbf{r}} \times \exp \left[\sum_{s=1}^n c_s \eta_s^* z_s w_s(\mathbf{r}) \right]. \quad (2.8)$$

As Ramakrishnan and Yussouff have shown,¹ one obtains a surprisingly good account of freezing into a bcc solid even at the level of a "one-order-parameter" theory, where $n=1$; i.e., only c_0 and c_1 are nonzero. For an account of freezing into an fcc solid, at least two order parameters are necessary, including the sets (111) and (311) which lie close to the first two peaks of $c(q)$, respectively. Calculations including as many as 50 order parameters have also been carried out using model correlation functions for hard spheres,^{10,11} Lennard-Jones systems,¹² and one-component plasma.¹³ Several authors¹⁴⁻¹⁷ have also investigated a variational approximation first used by Tarazona,¹⁸ where, instead of truncating the set of equations in reciprocal space as de-

scribed above, a periodic Gaussian ansatz is made for $\rho(\mathbf{r})$:

$$\rho(\mathbf{r})/\rho_l = \sum_{\mathbf{R}} A(\alpha/\pi)^{3/2} \exp[-\alpha(\mathbf{r}-\mathbf{R})^2] \quad (2.9)$$

and the free energy is minimized with respect to the three parameters A , α and the lattice constant a . Such investigations, which, in principle, use the full $c(q)$, have been carried out using the Ramakrishnan-Yussouff free-energy functional as well as other alternative forms^{15,16} for the functional, for hard spheres,^{13,14} Lennard-Jones systems,¹⁶ and the one-component plasma.¹⁷ Two-component systems, such as alloys¹⁹ and ionic solids,²⁰ have also been studied within the framework of the theory. For a recent review and reference to earlier work, see Refs. 11 and 21.

A. Extension to inhomogeneous crystals

In the sense of a mean-field approximation, it is reasonable to assume that the free-energy functional given in Eq. (2.2) not only describes the uniform crystal and the liquid, but also all possible intermediate density configurations corresponding to inhomogeneous crystals. Configurations that are important are those that correspond to local minima, in the space of density configurations, of $\Omega - \Omega_l$. The extension of the Ramakrishnan-Yussouff theory to cover such circumstances has been discussed by Oxtoby and co-workers in the contexts of the liquid-solid interface⁹ and a critical nucleus of the crystalline solid inside a supercooled liquid.²² Here we recapitulate the salient features of this extension.

Consider inhomogeneous solids which can be described by a density wave where the Fourier components are slowly varying spatially, i.e., density waves of the form

$$\rho(\mathbf{r}) = \rho_l \left[1 + \sum_{\mathbf{G}} \eta_{\mathbf{G}}(\mathbf{r}) e^{i\mathbf{G} \cdot \mathbf{r}} \right]. \quad (2.10)$$

For this to be meaningful, $\eta_{\mathbf{G}}(\mathbf{r})$ must vary slowly on the scale of the unit cell. Further, if we assume that the scale of variation of $\eta_{\mathbf{G}}(\mathbf{r})$ is small compared to the range of $c^{(2)}(\mathbf{r})$ then we can make a gradient expansion [of $\{\eta_{\mathbf{G}}(\mathbf{r}')\}$] in the nonlocal part of the free-energy functional (2.2) and write

$$\begin{aligned} \frac{\beta(\Omega - \Omega_l)}{\rho_l} &= \int d\mathbf{r} \left[1 + \sum_{\mathbf{G}} \eta_{\mathbf{G}}(\mathbf{r}) e^{i\mathbf{G} \cdot \mathbf{r}} \right] \ln \left[1 + \sum_{\mathbf{G}} \eta_{\mathbf{G}}(\mathbf{r}) e^{i\mathbf{G} \cdot \mathbf{r}} \right] - \sum_{\mathbf{G}} \int d\mathbf{r} \eta_{\mathbf{G}}(\mathbf{r}) e^{i\mathbf{G} \cdot \mathbf{r}} \\ &\quad - \frac{1}{2} \sum_{\mathbf{G}, \mathbf{G}'} \int d\mathbf{r} \int d\mathbf{r}' \eta_{\mathbf{G}}(\mathbf{r}) e^{i\mathbf{G} \cdot \mathbf{r}} c(\mathbf{r}-\mathbf{r}') e^{i\mathbf{G}' \cdot \mathbf{r}'} [\eta_{\mathbf{G}'}(\mathbf{r}') + (\mathbf{r}'-\mathbf{r})_i \partial_i \eta_{\mathbf{G}'}(\mathbf{r}') \\ &\quad + \frac{1}{2} (\mathbf{r}'-\mathbf{r})_i (\mathbf{r}'-\mathbf{r})_j \partial_i \partial_j \eta_{\mathbf{G}'}(\mathbf{r}') + \dots], \end{aligned} \quad (2.11)$$

where, as before, we have neglected $c^{(n)}$ for $n \geq 3$ and denoted

$$\rho_l c^{(2)}(\mathbf{r}-\mathbf{r}') \equiv c(\mathbf{r}-\mathbf{r}').$$

Now we invoke the assumed slow variation of $\eta_{\mathbf{G}}(\mathbf{r})$ to make a further "local" approximation as regards the first two terms, and write

$$\frac{\beta(\Omega - \Omega_l)}{\rho_l} = \int d\mathbf{r} \omega\{\eta_G(\mathbf{r})\} - \frac{1}{4} \int d\mathbf{r} \eta_0(\mathbf{r}) c_0'' \nabla^2 \eta_0(\mathbf{r}) - \frac{1}{2} \sum_{\mathbf{G}(\neq 0)} \int d\mathbf{r} \eta_{-\mathbf{G}}(\mathbf{r}) (-c_G^i \partial_i + \frac{1}{2} c_G^{ij} \partial_i \partial_j) \eta_G(\mathbf{r}) \quad (2.12)$$

in terms of $\omega\{\eta_G\}$, the free-energy functional for the homogeneous crystal, i.e., as given by the right-hand side of Eq. (2.5). Here c_G^i, c_G^{ij} are the moments of the direct correlation function, given by

$$\begin{pmatrix} c_G^i \\ c_G^{ij} \end{pmatrix} \equiv \int d\mathbf{r} e^{-i\mathbf{G}\cdot\mathbf{r}} \begin{pmatrix} r_i \\ r_i r_j \end{pmatrix} c(\mathbf{r}) = \begin{pmatrix} i \frac{\partial}{\partial G_i} \\ -\frac{\partial^2}{\partial G_i \partial G_j} \end{pmatrix} c(\mathbf{G}). \quad (2.13)$$

Since $c(\mathbf{G})$ is a function of $|\mathbf{G}|$ alone, these can be written as

$$c_G^i = i \frac{G_i}{|\mathbf{G}|} c_G', \quad c_G^{ij} = -\delta_{ij} \frac{c_G'}{|\mathbf{G}|} + \left[\frac{c_G'}{|\mathbf{G}|} - c_G'' \right] \frac{G_i G_j}{|\mathbf{G}|^2}. \quad (2.14)$$

The extremization of the free-energy functional (2.12) with respect to $\eta_G(\mathbf{r})$ and $\eta_0(\mathbf{r})$ gives us the following coupled nonlinear second-order differential equations:

$$\frac{1}{2} c_0'' \nabla^2 \eta_0(\mathbf{r}) = \frac{\partial \omega\{\eta_G(\mathbf{r})\}}{\partial \eta_0} \equiv -U_0\{\eta_G(\mathbf{r})\}, \quad (2.15a)$$

$$\begin{aligned} \frac{1}{2} (-c_G^i \partial_i + \frac{1}{2} c_G^{ij} \partial_i \partial_j) \eta_G(\mathbf{r}) &\equiv \frac{\partial \omega\{\eta_G(\mathbf{r})\}}{\partial \eta_{-\mathbf{G}}} \\ &\equiv -U_{-\mathbf{G}}\{\eta_G(\mathbf{r})\}. \end{aligned} \quad (2.15b)$$

By considering the freezing of a crystal in the presence of a periodic potential, it is not hard to see that $U_0\{\eta_G\}/\beta$ and $U_G\{\eta_G\}/\beta$ can be interpreted as the Fourier components of an external potential that would be required to stabilize any given values of $\{\eta_G\}$ in a homogeneous situation. Hence, they are also determined implicitly as solutions of the equations [cf. (2.1) and (2.4)]

$$1 + \sum_{\mathbf{G}} \eta_G e^{i\mathbf{G}\cdot\mathbf{r}} = \exp \left[(c_0 \eta_0 - U_0) + \sum_{\mathbf{G}} (c_G \eta_G - U_G) e^{i\mathbf{G}\cdot\mathbf{r}} \right]. \quad (2.16)$$

[Differentiation of the right-hand side of Eq. (2.5) with respect to η_G yields a set of equations which is equivalent.] $\omega\{\eta_G\}$ can be expressed in terms of the functions U_G as

$$\omega = (c_0 - 1) \eta_0 - U_0 + \frac{1}{2} \sum_{\mathbf{G}} c_G |\eta_G|^2 - \sum_{\mathbf{G}} \eta_G U_G. \quad (2.17)$$

In any particular application, suppose that, similar to the case of the uniform crystal, we take $c_G, c_G^i,$ and c_G^{ij} to be nonzero only for the first $(n+1)$ sets of reciprocal-lattice vectors (including $G=0$). Then the differential equations (2.15) have to be solved only for the $(1 + \sum_{s=1}^n z_s)$ variables $\eta_0(\mathbf{r})$ and $\{\eta_{G_i^{(s)}}(\mathbf{r})\}$. U_0 and $U_{G_i^{(s)}}$ can now be regarded as functions only of these variables and are determined as solutions of the $(n+1)$ coupled equations [obtained from (2.16)]:

$$\begin{pmatrix} 1 + \eta_0 \\ \eta_{G_i^{(s)}} \end{pmatrix} = e^{(c_0 \eta_0 - U_0)} \int d\mathbf{r} \begin{pmatrix} 1 \\ e^{-i\mathbf{G}_i^{(s)} \cdot \mathbf{r}} \end{pmatrix} \exp \left[\sum_{t=1}^n \sum_{j=1}^{z_t} (c_t \eta_{G_j^{(t)}} - U_{G_j^{(t)}}) e^{i\mathbf{G}_j^{(t)} \cdot \mathbf{r}} \right]. \quad (2.18)$$

The remaining $\{\eta_G(\mathbf{r})\}$, i.e., corresponding to those reciprocal-lattice vectors (RLV's) for which $c_G, c_G^i,$ and c_G^{ij} have been set equal to zero, are determined as the zeros of the corresponding potentials $\{U_G(\mathbf{r})\}$. Hence, from (2.16)

$$\eta_G(\mathbf{r}) = e^{(c_0 \eta_0 - U_0)} \int^{\text{cell}} d\mathbf{r} e^{-i\mathbf{G}\cdot\mathbf{r}} \exp \left[\sum_{t=1}^n \sum_{j=1}^{z_t} (c_t \eta_{G_j^{(t)}} - U_{G_j^{(t)}}) e^{i\mathbf{G}_j^{(t)} \cdot \mathbf{r}} \right], \quad (2.19)$$

where the right-hand side is first obtained as a function of η_0 and $\{\eta_{G_i^{(s)}}\}$ and then evaluated at the $\eta_0(\mathbf{r})$ and $\{\eta_{G_i^{(s)}}(\mathbf{r})\}$ that solve the differential equations. In other words, these $\{\eta_G\}$ are the same functions (locally) of $\{c_s \eta_{G_i^{(s)}}(\mathbf{r}) - U_{G_i^{(s)}}(\mathbf{r})\}$ and $[c_0 \eta_0(\mathbf{r}) - U_0(\mathbf{r})]$ as they are of $\{c_s \eta_{G_i^{(s)}}\}$ and η_0 in the homogeneous case.

The minimized free energy for the inhomogeneous case, Ω_{inh} , is also straightforward to write down. One can, starting from (2.12), make use of the fact that η_0 and $\{\eta_{G_i^{(s)}}\}$ satisfy the differential equations (2.15), and show that

$$\begin{aligned} \frac{\beta(\Omega_{\text{inh}} - \Omega_l)}{\rho_l} &= \int d\mathbf{r} \left[(c_0 - 1) \eta_0 - U_0 \right. \\ &\quad \left. + \frac{1}{2} \sum_{\mathbf{G}} \eta_{-\mathbf{G}}(\mathbf{r}) [c_G \eta_G(\mathbf{r}) - U_G] \right]. \end{aligned} \quad (2.20)$$

III. SCHEME FOR DISLOCATIONS IN GENERAL

In general, $\{\eta_G(\mathbf{r})\}$ are complex and can be represented as

$$\{\eta_G(\mathbf{r})\} = \{\mu_G(\mathbf{r}) \exp[i\phi_G(\mathbf{r})]\}.$$

Dislocations are topological defects and we characterize them by the condition that the phases $\{\phi_G(\mathbf{r})\}$ may change by integral multiples of 2π on going around paths encircling the dislocation, i.e., $\oint d\phi_G = 2\pi n_G$. This condition is equivalent to the more familiar Burgers condition. For, even in the presence of the dislocation, and the accompanying strain field, the solid will be locally periodic, asymptotically far from the core of the dislocation. Locally, the effective reciprocal-lattice vectors are $\mathbf{G} + \nabla\phi_G$ and these can always be linearly related to \mathbf{G} . Hence, we can argue that

$$\phi_G = \mathbf{G} \cdot \mathbf{u}(r), \quad (3.1)$$

where $\mathbf{u}(r)$ can be interpreted as the local displacement or deformation of the solid. The topological condition

$$\oint d\phi_G = 2\pi n_G = \mathbf{G} \cdot \oint d\mathbf{u} \implies \oint d\mathbf{u} = \mathbf{b}, \quad (3.2)$$

where \mathbf{b} must be a vector of the direct lattice. This is the familiar condition, and \mathbf{b} is nothing but the Burgers vector that characterizes the dislocation.

As is well known,⁴ the geometry and configuration of dislocations completely determine the singular part of the displacement field. For example, for a screw dislocation along the z axis, with the Burgers vector $\mathbf{b} = b\hat{z}$, we have

$$\mathbf{u}^{(\text{sing})}(r) = b\hat{z}\phi/2\pi, \quad (3.3)$$

where ϕ is the azimuthal angle, and for an edge dislocation along the z axis with the Burgers vector $\mathbf{b} = b\hat{x}$, we have

$$\mathbf{u}^{(\text{sing})}(r) = b\hat{x}\phi/2\pi. \quad (3.4)$$

Then the singular part of the phases is

$$\phi_G^{(\text{sing})}(\mathbf{r}) = \mathbf{G} \cdot \mathbf{u}^{(\text{sing})}(r). \quad (3.5)$$

Given these, we still need to determine the regular parts of the phases $\{\phi_G(\mathbf{r})\}$ as well as the amplitudes $\{\mu_G(\mathbf{r})\}$ to obtain the dislocation structure and energetics. For this, we use the framework developed in Sec. II for handling general inhomogeneous situations, which depends on the gradient expansion and local approximation. In other words the regular parts of the phases and the amplitudes are obtained by solving the set of nonlinear differential equations (2.15) with appropriate boundary conditions. These boundary conditions are the following: (i) as we go away from the dislocation, i.e., as $r \rightarrow \infty$, $\{\mu_G(r)\} \rightarrow \{\mu_G^*\}$ of the underformed solid, and (ii) at the core of the dislocation, i.e., as $r \rightarrow 0$, $\{\mu_G\} \rightarrow 0$ for those \mathbf{G} for which $\mathbf{G} \cdot \mathbf{b} \neq 0$; that is, the \mathbf{G} for which $\oint d\phi_G \neq 0$ around paths encircling the dislocation.

We thus have a prescription for calculating the free

energies of dislocations, the structure of their cores, the core energy, etc. The above scheme is analogous to the calculation of vortex structure and energetics in a superconductor or superfluid within the framework of a Landau-Ginzburg theory.²³

IV. APPLICATION TO THE $(a/2)[111]$ SCREW DISLOCATION IN A bcc SOLID

We now apply the above scheme to investigate in detail the structure of the $\frac{1}{2}a(1,1,1)$ screw dislocation in a bcc solid.

We have chosen to study the $\frac{1}{2}a(1,1,1)$ screw dislocation because this is the simplest of the dislocation problems; for, the differential equations for $\{\mu_G\}$ in this case can be reduced to ordinary differential equations. All edge dislocations, as also screw dislocations in other directions, lead to partial-differential equations which are much more difficult to solve. At the same time, $\frac{1}{2}a(1,1,1)$ being the smallest possible Burgers vector, dislocations with this Burgers vector have the least energy ($E_{\text{disl}} \propto b^2$) and are, therefore, the ones most likely to appear in actual systems. They, hence, play an important role in determining the mechanical properties of bcc solids, and have been studied extensively by atomistic theories.⁵⁻⁷

The system of ordinary differential equations for the $\frac{1}{2}a(1,1,1)$ screw dislocation in a bcc solid alluded to above are still sufficiently complicated to present a hard numerical problem. We have, hence, made the further simplifying assumption of neglecting all but $c^{(2)}(q=0)$ and the first peak of $c^{(2)}(q)$. That is, in Eqs. (2.15) and (2.16), only $c_0^{(2)}$, $c_{G^{(1)}}^{(2)}$, and $c_{G^{(1)}}^{(2)''}$, where $G^{(1)}$ is the first set of reciprocal-lattice vectors, are taken to be nonzero; we will denote these by c_0 , c_1 , and c_1'' , respectively. As mentioned earlier, it has been shown that even within this approximation, one gets a reasonable zeroth-order description of the liquid-bcc transition,¹ the elastic properties of the bcc solid,^{3,8} etc. Furthermore, this is the only approximation within which any inhomogeneous problems such as solid-liquid interface or nucleation have been tackled.⁹ We discuss the limitations of the various approximations we have made, in Sec. VI.

The effect of the above approximation is that the differential equations (2.15) have to be set up and solved only for the $\{\eta_{G^{(1)}}\}$ for the first set of reciprocal-lattice vectors. The remaining $\{\eta_G\}$ will be determined in terms of these by algebraic equations, as described in Sec. II.

The symmetries inherent in the present problem permit its further simplification as follows. Depending on the value of the singular part of the phase $\phi_G = (\mathbf{G} \cdot \mathbf{b}/2\pi)\phi$, where ϕ is the azimuthal angle around the $[111]$ direction and $\mathbf{b} = \frac{1}{2}a(\hat{x} + \hat{y} + \hat{z})$, the 12 smallest reciprocal-lattice vectors fall into three classes:

- (i) $\mathbf{G}/(2\pi/a) = (1, 1, 0), (1, 0, 1), (0, 1, 1), \quad \phi_G = +\phi$
- (ii) $\mathbf{G}/(2\pi/a) = (-1, -1, 0), (-1, 0, -1), (0, -1, -1), \quad \phi_G = -\phi$
- (iii) $\mathbf{G}/(2\pi/a) = (1, -1, 0), (1, 0, -1), (0, 1, -1), (-1, 1, 0), (-1, 0, 1), (0, -1, 1), \quad \phi_G = 0.$

$\mu_G^{(1)}$ for G within each class will be the same by symmetry. Consequently, there will be only three distinct amplitudes which we denote $\mu_{1,+}$, $\mu_{1,-}$, and $\mu_{1,0}$, and, correspondingly, three distinct Fourier components of the potential which we denote $U_{1,+}$, $U_{1,-}$, and $U_{1,0}$. Furthermore, from Eqs. (2.15) it is clear that we can set $U_{1,+} = U_{1,-}$ and $\mu_{1,+} = \mu_{1,-}$. Finally, from the symmetry of the problem, it is not hard to see that $\mu_{1,+}$, $\mu_{1,-}$, and $\mu_{1,0}$ will be functions only of the radial distance r from the axis of the dislocation; that is,

$$\begin{aligned}\eta_{1,+}(\mathbf{r}) &= \mu_{1,+}(r)e^{i\phi}, \\ \eta_{1,-}(\mathbf{r}) &= \mu_{1,-}(r)e^{-i\phi}, \\ \eta_{1,0}(\mathbf{r}) &= \mu_{1,0}(r).\end{aligned}\quad (4.2)$$

Hereafter we will use the following notation for convenience:

$$\begin{aligned}\mu_1 &\equiv \mu_{1,+}, \mu_{1,-}, \quad \mu_2 \equiv \mu_{1,0} \\ U_1 &= U_{1,+}, U_{1,-}, \quad U_2 = U_{1,0}.\end{aligned}\quad (4.3)$$

Thus, the set of nonlinear partial-differential equations (2.15) can be reduced to just two coupled ordinary differential equations for the amplitudes μ_1 and μ_2 :

$$c_1'' \left[\frac{d^2\mu_1}{dr^2} + \frac{1}{r} \frac{d\mu_1}{dr} - \frac{\mu_1}{r^2} \right] = 12U_1(\mu_1, \mu_2), \quad (4.4a)$$

$$c_1'' \left[\frac{d^2\mu_2}{dr^2} + \frac{1}{r} \frac{d\mu_2}{dr} \right] = 4U_2(\mu_1, \mu_2). \quad (4.4b)$$

Here, U_1 and U_2 have been treated to be functions of μ_1 and μ_2 alone, and not of η_0 too. This is possible because η_0 can be determined in terms of μ_1 and μ_2 via Eq. (2.15a) which, as a result of setting $c_0'' = 0$, reduces to the algebraic equation $U_0 = 0$. When this is used in the first of Eqs. (2.18), we get

$$1 + \eta_0 = e^{c_0\eta_0} \int d\mathbf{r} \exp \left[\sum_{j=1}^6 (c_1\mu_1 - U_1) \exp(i\mathbf{G}_j^{(1)} \cdot \mathbf{r}) + \sum_{j=7}^{12} (c_1\mu_2 - U_2) \times \exp(i\mathbf{G}_j^{(1)} \cdot \mathbf{r}) \right]. \quad (4.5)$$

Generally, the value of c_0 is found to be very large and negative. So we can make a large c_0 expansion in the above equations, and obtain η_0 explicitly to be

$$\eta_0 = -\ln\phi_0 / (1 - c_0), \quad (4.6)$$

where

$$\phi_0 = \frac{1}{v} \int^{\text{cell}} d\mathbf{r} \exp[6(c_1\mu_1 - U_1)w_1(\mathbf{r}) + 6(c_1\mu_2 - U_2)w_2(\mathbf{r})], \quad (4.7)$$

$$\begin{aligned}w_1(\mathbf{r}) &= \frac{1}{6} \sum_{\substack{\mathbf{G}_j^{(1)} \in \text{class(i)} \\ \text{and(ii)}}} \exp(i\mathbf{G}_j^{(1)} \cdot \mathbf{r}) \\ &= \frac{1}{3} \left[\cos \left[\frac{2\pi}{a}(x+y) \right] + \cos \left[\frac{2\pi}{a}(y+z) \right] + \cos \left[\frac{2\pi}{a}(z+x) \right] \right],\end{aligned}\quad (4.8a)$$

$$\begin{aligned}w_2(\mathbf{r}) &= \frac{1}{6} \sum_{\mathbf{G}_j^{(1)} \in \text{class(iii)}} \exp(i\mathbf{G}_j^{(1)} \cdot \mathbf{r}) \\ &= \frac{1}{3} \left[\cos \left[\frac{2\pi}{a}(x-y) \right] + \cos \left[\frac{2\pi}{a}(y-z) \right] + \cos \left[\frac{2\pi}{a}(z-x) \right] \right]\end{aligned}\quad (4.8b)$$

[refer to equation (4.1) for classes (i), (ii), and (iii)]. Now it is easy to see that the functions U_1 and U_2 have to be determined numerically from the two equations [obtained by using Eqs. (4.5) and (4.6) in Eq. (2.18)]:

$$\begin{bmatrix} \mu_1 \\ \mu_2 \end{bmatrix} = \frac{1}{\phi_0} \left[1 + \frac{\ln\phi_0}{1 - c_0} \right] \frac{1}{v} \int^{\text{cell}} d\mathbf{r} \begin{bmatrix} w_1(\mathbf{r}) \\ w_2(\mathbf{r}) \end{bmatrix} \exp[6(c_1\mu_1 - U_1)w_1(\mathbf{r}) + 6(c_1\mu_2 - U_2)w_2(\mathbf{r})]. \quad (4.9)$$

The differential equations (4.4) have to be solved with the following boundary conditions for μ_1 and μ_2 .

(i) As $r \rightarrow \infty$, $\mu_1, \mu_2 \rightarrow \mu^*$, the value of μ for the uniform solid for the first set of reciprocal-lattice vectors $\{\mathbf{G}^{(1)}\}$.

(ii) $\{\eta_G(\mathbf{r})\}$ must be regular at $r = 0$. Hence, as $r \rightarrow 0$, we expect that $\mu_1 \rightarrow 0$ because the phases of $\eta_{1,+}$ and

$\eta_{1,-}$ are singular at $r = 0$. In contrast, $d\mu_2/dr \rightarrow 0$ but $\mu_2 \rightarrow \text{const}$ as $r \rightarrow 0$.

In principle, the above boundary conditions are sufficient for solving the differential equations (4.4) numerically. In practice we have found it useful to work out, explicitly, the asymptotic behavior of μ_1 and μ_2 as $r \rightarrow 0$ and $r \rightarrow \infty$, which can be done analytically. The

results are [with $\bar{r} \equiv r / (|c_1''|)^{1/2}$] (i) as $\bar{r} \rightarrow 0$,

$$\begin{aligned}\mu_1 &= a_1 \bar{r} - 4U_1(0, a_2) \bar{r}^2, \\ \mu_2 &= a_2 - U_2(0, a_2) \bar{r}^2,\end{aligned}\quad (4.10)$$

where a_1, a_2 are constants that are to be determined by solving the boundary-value problem; (ii) as $\bar{r} \rightarrow \infty$,

$$\begin{aligned}\mu_1 &= \mu^* - \frac{(\partial U_2 / \partial \mu_2)^* \mu^*}{\mathcal{D}} \frac{1}{\bar{r}^2} + \dots, \\ \mu_2 &= \mu^* - \frac{(\partial U_2 / \partial \mu_1)^* \mu^*}{\mathcal{D}} \frac{1}{\bar{r}^2} + \dots,\end{aligned}\quad (4.11)$$

where the * on the derivatives means that these are to be evaluated for $\mu_1, \mu_2 = \mu^*$ and

$$\mathcal{D} = \left[\frac{\partial U_1}{\partial \mu_1} \frac{\partial U_2}{\partial \mu_2} - \frac{\partial U_1}{\partial \mu_2} \frac{\partial U_2}{\partial \mu_1} \right] \Big|_{\mu_1, \mu_2 = \mu^*}.$$

The $1/\bar{r}^2$ dependence of μ_1 and μ_2 as $r \rightarrow \infty$ is consistent with what is expected for an elastically distorted solid with the displacement field $\mathbf{u} = \mathbf{b}\phi/2\pi$ (see Sec. V).

V. DETAILS OF THE CALCULATIONS: USE OF THE MOLECULAR FIELD

The boundary-value problem defined by Eqs. (4.4), (4.10), and (4.11) is to be solved numerically. Typically this is done using shooting and matching methods or iteration methods. For this purpose we need the functions $U_1(\mu_1, \mu_2)$ and $U_2(\mu_1, \mu_2)$ for a whole range of values of μ_1 and μ_2 . Since U_1 and U_2 can be obtained only by numerically solving the coupled nonlinear equations, this proves to be very expensive computationally.

We have found that a nice way of avoiding this computational expense is to work with $\{\xi_G\}$, the Fourier components of the molecular field rather than with $\{\mu_G\}$. We define them by

$$\xi_G \equiv c_G \mu_G - U_G. \quad (5.1)$$

In our case we need only two molecular fields:

$$\xi_1 \equiv c_1 \mu_1 - U_1 \quad \text{and} \quad \xi_2 \equiv c_1 \mu_2 - U_2. \quad (5.2)$$

Now consider expressing U_1, U_2 and μ_1, μ_2 as functions of ξ_1 and ξ_2 . The equations determining these are clearly

$$\begin{pmatrix} \mu_1(\xi_1, \xi_2) \\ \mu_2(\xi_1, \xi_2) \end{pmatrix} = \frac{1}{\phi_0} \left[1 + \frac{\ln \phi_0}{1 - c_0} \right] \frac{1}{v} \int^{\text{cell}} d\mathbf{r} \begin{pmatrix} w_1(\mathbf{r}) \\ w_2(\mathbf{r}) \end{pmatrix} \exp[6\xi_1 w_1(\mathbf{r}) + 6\xi_2 w_2(\mathbf{r})], \quad (5.3)$$

$$U_1(\xi_1, \xi_2) = c_1 \mu_1(\xi_1, \xi_2) - \xi_1, \quad U_2(\xi_1, \xi_2) = c_1 \mu_2(\xi_1, \xi_2) - \xi_2, \quad (5.4)$$

with

$$\phi_0(\xi_1, \xi_2) \equiv \frac{1}{v} \int^{\text{cell}} d\mathbf{r} \exp[6\xi_1 w_1(\mathbf{r}) + 6\xi_2 w_2(\mathbf{r})]. \quad (5.5)$$

Note that the computation of U_1, U_2 or μ_1, μ_2 as functions of ξ_1, ξ_2 does not involve solving equations but only needs evaluation of integrals. We have found it computationally advantageous to avoid even the latter by developing ϕ_0 as a power series in ξ_1 and ξ_2 , and computing μ_1 and μ_2 as ratios of two series:

$$\mu_1 = \frac{1}{6} \frac{(\partial \phi_0 / \partial \xi_1)}{\phi_0} \left[1 + \frac{\ln \phi_0}{1 - c_0} \right], \quad \mu_2 = \frac{1}{6} \frac{(\partial \phi_0 / \partial \xi_2)}{\phi_0} \left[1 + \frac{\ln \phi_0}{1 - c_0} \right]. \quad (5.6)$$

The differential equations (4.4) for $\mu_1(r)$ and $\mu_2(r)$ can be recast as the following equations for $\xi_1(\bar{r})$ and $\xi_2(\bar{r})$:

$$\begin{pmatrix} \mu_{11} & \mu_{12} \\ \mu_{21} & \mu_{22} \end{pmatrix} \begin{pmatrix} \xi_1'' \\ \xi_2'' \end{pmatrix} = \begin{pmatrix} -\mu_{111} \xi_1'^2 - 2\mu_{112} \xi_1' \xi_2' - \mu_{122} \xi_2'^2 - \mu_{11} \xi_1' / x - \mu_{12} \xi_2' / x + \mu_1 / x^2 - 12c_1 \mu_1 + 12\xi_1 \\ -\mu_{211} \xi_1'^2 - 2\mu_{212} \xi_1' \xi_2' - \mu_{222} \xi_2'^2 - \mu_{21} \xi_1' / x - \mu_{22} \xi_2' / x - 4c_1 \mu_2 + 4\xi_2 \end{pmatrix}. \quad (5.7)$$

Here

$$\mu_{ij} \equiv \partial \mu_i / \partial \xi_j, \quad \mu_{ijk} \equiv \partial^2 \mu_i / \partial \xi_j \partial \xi_k, \quad i, j, k = 1, 2$$

and

$$\xi_i' \equiv d\xi_i / d\bar{r}, \quad \xi_i'' \equiv d^2 \xi_i / d\bar{r}^2.$$

The boundary conditions for $\xi_1(\bar{r})$ and $\xi_2(\bar{r})$ are as follows:

$$(i) \text{ as } \bar{r} \rightarrow 0, \quad \xi_1(\bar{r}) \rightarrow 0 \text{ and } d\xi_2(\bar{r})/d\bar{r} \rightarrow 0, \quad (5.8)$$

$$(ii) \text{ as } \bar{r} \rightarrow \infty, \quad \xi_1(\bar{r}) \rightarrow \xi_1^* (= c_1 \mu^*) \text{ and } \xi_2(\bar{r}) \rightarrow \xi_2^*. \quad (5.9)$$

The asymptotic behavior of $\xi_1(\bar{r})$ and $\xi_2(\bar{r})$ can also be obtained. Close to the dislocation core, i.e., as $\bar{r} \rightarrow 0$, the behavior is [compare to Eq. (4.10)]

$$\begin{aligned}\xi_1(\bar{r}) &= b_1 \bar{r} + b_3 \bar{r}^2 + O(\bar{r}^3), \\ \xi_2(\bar{r}) &= b_2 + b_4 \bar{r}^2,\end{aligned}\quad (5.10)$$

where b_1 and b_2 are related to the constants a_1 and a_2 in Eq. (4.10), and b_3, b_4 are determined in terms of b_1 and b_2 via the equations

$$\begin{aligned}6\mu_{11}b_3 + 6\mu_{12}b_4 &= -3\mu_{11}b_1^2, \\ 4\mu_{21}b_3 + 4\mu_{22}b_4 &= -2\mu_{21}b_1^2 - 4c_1\mu_2 + 4b_2\end{aligned}\quad (5.11)$$

obtained by substituting the expressions (5.10) in Eqs. (5.7). Here $\mu_i, \mu_{ij}, \mu_{ijk}$ are evaluated at $\xi_1=0, \xi_2=b_2$. The coefficient b_3 turns out to be zero,²⁴ and then the second equation in (5.11) determines b_4 . In the region asymptotically far from the dislocation axis, i.e., as $\bar{r} \rightarrow \infty$, we can show that

$$\begin{aligned}\xi_1(\bar{r}) &= \xi^* + d_1^{(2)}/\bar{r}^2 + d_1^{(4)}/\bar{r}^4 + \dots, \\ \xi_2(\bar{r}) &= \xi^* + d_2^{(2)}/\bar{r}^2 + d_2^{(4)}/\bar{r}^4 + \dots.\end{aligned}\quad (5.12)$$

Here

$$d_1^{(2)} = \frac{4\mu^*(c_1\mu_{22}-1)}{48[(c_1\mu_{11}-1)(c_1\mu_{22}-1)-c_1^2\mu_{12}^2]}$$

and

$$d_2^{(2)} = \frac{-4\mu^*c_1\mu_{21}}{48[(c_1\mu_{11}-1)(c_1\mu_{22}-1)-c_1^2\mu_{12}^2]}.$$

Here the μ_{ij} are evaluated at $\xi_1=\xi_2=\xi^*$. We have also

$$\begin{aligned}\frac{\Omega_s + \text{disl} - \Omega_l}{\rho_l k_B T} &= 2\pi L |c_1''| \int_0^R dr r [(c_0-1)\eta_0(r) + \frac{1}{2}c_0\eta_0^2(r) + \frac{1}{2}z_1c_1\mu_1^2(r) + \frac{1}{2}z_2c_1\mu_2^2(r) \\ &\quad - \frac{1}{2}z_1\mu_1(r)U_1(\mu_1, \mu_2) - \frac{1}{2}z_2\mu_2(r)U_2(\mu_1, \mu_2)] \\ &= 2\pi L |c_1''| \int_0^R dr r [(c_0-1)\eta_0(r) + \frac{1}{2}c_0\eta_0^2(r) + \frac{1}{2}z_1\mu_1(r)\xi_1(r) + \frac{1}{2}z_2\mu_2(r)\xi_2(r)],\end{aligned}\quad (5.15)$$

where R is the radial size of the solid and L the axial size. Then the free energy of the dislocation is given by

$$\frac{F_{\text{disl}}}{\rho_l k_B T} = \frac{\Omega_s + \text{disl} - \Omega_s}{\rho_l k_B T} = \frac{\Omega_s + \text{disl} - \Omega_l}{\rho_l k_B T} - \frac{\Omega_s - \Omega_l}{\rho_l k_B T},\quad (5.16)$$

where

$$\begin{aligned}\frac{\Omega_s - \Omega_l}{\rho_l k_B T} &= 2\pi L |c_1''| [(c_0-1)\eta_0^* + \frac{1}{2}c_0\eta_0^{*2} + \frac{1}{2}z_1c_1\mu_1^* \\ &\quad + \frac{1}{2}z_2c_1\mu_2^*] \int_0^R r dr.\end{aligned}\quad (5.17)$$

Now $\Omega_s - \Omega_l$ is nonzero at temperatures less than T_m

calculated $d_1^{(4)}$ and $d_2^{(4)}$, but do not display their lengthy expressions here.

To solve the differential equations (5.7), we follow the standard technique of casting them into a system of four first-order equations by introducing the derivative functions $\xi_3 \equiv \xi_1'$ and $\xi_4 \equiv \xi_2'$. This system is then solved using the NAG routine DO2RAF (which uses a variable-order, variable-step-size finite-difference method with deferred corrections and Newton iteration) in a range $\bar{r}_{\min} < \bar{r} < \bar{r}_{\max}$. Here \bar{r}_{\min} and \bar{r}_{\max} have to be so chosen that for $\bar{r} < \bar{r}_{\min}$ the solution (5.10) is valid and for $\bar{r} > \bar{r}_{\max}$ the asymptotic solution (5.12) holds. The boundary condition at \bar{r}_{\min} can be reduced to the following two equations by eliminating the unknown constants b_1 and b_2 in Eq. (5.10):

$$\begin{aligned}\xi_1(\bar{r}_{\min}) &= \bar{r}_{\min}\xi_3(\bar{r}_{\min}), \\ \xi_4(\bar{r}_{\min}) &= 2\bar{r}_{\min}b_4[\xi_3(\bar{r}_{\min}), \xi_2(\bar{r}_{\min}) - \frac{1}{2}\xi_4(\bar{r}_{\min})\bar{r}_{\min}],\end{aligned}\quad (5.13)$$

where the function $b_4[b_1, b_2]$ was defined in (5.11). At $\bar{r} = \bar{r}_{\max}$ we can simply use expressions (5.12) for $\xi_1(\bar{r}_{\max})$ and $\xi_2(\bar{r}_{\max})$.

Once the functions $\xi_1(\bar{r})$ and $\xi_2(\bar{r})$ are known, various properties of the dislocation, such as the local mean density change $\eta_0(\bar{r})$ in the distorted solid, the dislocation core energy, and the core structure, can be obtained.

The local density change $\eta_0(\bar{r})$ of the distorted solid with respect to the liquid is obtained simply as [cf. Eq. (4.6)]

$$\eta_0(\bar{r}) = \ln \phi_0(\xi_1(\bar{r}), \xi_2(\bar{r})) / (1 - c_0). \quad (5.14)$$

The excess free energy of the distorted solid (i.e., the solid with the dislocation) over the uniform liquid can be obtained from Eq. (2.20), now reexpressible as

(the freezing temperature). Here, η_0^* is the value of η_0 in the uniform solid. Using the asymptotic solutions for ξ_1 and ξ_2 for large r [sufficiently large that the terms of $O(1/r^4)$ in (5.12) are negligible], it is straightforward to see that the dominant contribution to the dislocation free energy from the asymptotic region is

$$(\lambda b^2/4\pi) \int_{R_1}^R \frac{dr}{r} = (\lambda b^2/4\pi) \ln(R/R_1). \quad (5.18)$$

Here

$$\lambda = \rho_l k_B T |c_1''| |G_1|^2 \mu^{*2}/3,$$

which is nothing but the shear elastic constant (appropriate to the present case) in the one-order-parameter approximation of the density-wave theory, as

has been calculated earlier by other methods.^{3,8} Thus our theory for the dislocation agrees with the elastic continuum description in the asymptotic region.

It is conventional to express the full free energy for the dislocation, including the contribution from the nonasymptotic region, in the form

$$F_{\text{disl}}/L = (\lambda b^2/4\pi) \ln(\alpha R/b). \quad (5.19)$$

Then α , which is a measure of the core energy, can be calculated. The details are given in the next section.

We can also easily obtain the detailed structure of the dislocation, since, in terms of the molecular fields, the density distribution is just [cf. Eq. (2.16)]

$$\begin{aligned} \frac{\rho_D(\mathbf{r})}{\rho_l} &= \exp \left[\xi_0(\mathbf{r}) + \sum_{G(\neq 0)} \xi_G(\mathbf{r}) e^{iG \cdot \mathbf{r}} \right] \\ &= \exp [c_0 \eta_0(\bar{r}) + 6\xi_1(\bar{r}) w_1(\mathbf{r}) + 6\xi_2(\bar{r}) w_2(\mathbf{r})], \end{aligned} \quad (5.20)$$

which can be computed for any choice of the placing of the dislocation axis relative to the unit cell of the lattice.

VI. RESULTS

In this section we present and discuss our results for the order-parameter profiles, the dislocation core energy, and the core structure. We have performed the calculations for sodium at two temperatures, the melting temperature T_m and at $T_m - 100$ K (at ambient pressure). Temperature enters our theory via the parameters a , c_0 , c_1 , and c_1'' which are temperature dependent. Of these, the role of the parameters a and c_1'' is trivial in that they enter the theory as scale factors. However, the dependence on c_0 and c_1 of the various properties of the dislocation is nontrivial.

For the purposes of our calculations, we need the values of a , c_0 , c_1 , and c_1'' at freezing and in the supercooled, metastable liquid at the temperature of interest. Unfortunately, such detailed information about the liquid structure factor or direct correlation function is not available. We have relied on experimental data for sodium extrapolated into the supercooled region from data taken at and above the freezing temperature, and used earlier in the context of the liquid-solid interface⁹ and nucleation.²² The data are summarized in Table I. They are expected to be accurate up to 5%.

A. Order-parameter profiles

The profiles of ξ_1 , ξ_2 , and η_0 as a function of the reduced radial variable $\bar{r} [= r / (|c_1''|)^{1/2}]$ are shown in Fig. 1 for $T = T_m$ (= 371 K for Na), and in Fig. 2 for $T = T_m - 100$ K (= 271 K). It is worth noting some features of our results for the profiles. If we estimate the radial extent of the dislocation core as the radial distance at which $\xi_1(\bar{r})$ attains 95% of its value in the uniform solid, then, in reduced units, we get a width of about 3.1 at the melting temperature and a much lower value of 2.4 at the lower temperature. However, since $|c_1''|$ can be expected to be higher at the lower temperature, in real units the difference in core widths is probably much less. To get an idea of the actual widths, note that at $T = T_m$, $(|c_1''|)^{1/2}$ and a are almost the same for sodium, and hence \bar{r} is roughly r in units of the bcc lattice constant. Using the value of a for Na, this corresponds to a width of about 14 Å.

Further, the core of the dislocation is somewhat liquidlike, in that η_0 , the fractional mean density change at $x=0$, is only 0.015 (0.017) at $T = T_m$ ($T_m - 100$ K), which is about one-third of its value in the uniform solid.

Another notable feature is that as one moves outward from the core, the η_0 profile grows to its uniform solid value slower than the ξ_1, ξ_2 profiles do to theirs.

B. Dislocation core energy

In order to calculate α [cf. Eq. (5.19)], we have calculated F_{disl} (the full free energy for the dislocation) as the sum of three contributions: (i) from the near region, $0 < r < r_{\text{max}}$, using the numerical solutions for ξ_1 and ξ_2 , (ii) from the intermediate region, $r_{\text{max}} < r < R_1$, using the asymptotic solution for ξ_1 and ξ_2 given by (5.12), and (iii) from the far region, $R_1 < r$, where the contribution to the free energy is given by Eq. (5.18). We have checked that the result is independent of the choice of R_1 .

We get for α , the measure of the core energy, the following values:

- (i) At $T = T_m$ (= 371 K for Na)

$$\begin{aligned} \alpha &= 1.94a / (|c_1''|)^{1/2} \\ &= 1.85 \end{aligned}$$

(using the values of parameters given in Table I).

- (ii) At $T = T_m - 100$ K (= 271 K)

$$\alpha = 2.48a / (|c_1''|)^{1/2}.$$

TABLE I. Values of parameters for sodium (taken from Refs. 1 and 21).

T (K)	c_0	c_1	ξ^*	η_0^*	c_1'' (Å ²)	a (Å)
371	-40.0 ^a	0.687 ^b	0.484 ^b	0.049 ^b	-20.6 ^a	4.313 ^a
271	-49.96 ^a	0.717 ^a	0.533 ^b	0.047 ^b		4.276 ^a

^aInput data taken from experiments.

^bObtained from theory.

As one might have expected, the core energy increases with decreasing temperature. The only other calculation of the dislocation core energy is the atomistic description^{5,7} (i.e., $T=0$) which gives $\alpha \sim 4-5$.

C. Atomic configuration of the dislocation

Here we discuss the atomic configuration of the dislocation for a particular choice of the position of its axis, namely, when it passes through the center of a triangle in the triangular lattice obtained by projection of the bcc lattice on its (111) plane (see Fig. 4). The z axis is chosen to be along the dislocation axis, i.e., in the [111] direction, and the x and y axes are as shown in the figure. In this coordinate system, the functions $w_1(\mathbf{r})$ and $w_2(\mathbf{r})$ which appear in Eq. (5.20) are given by

$$w_1(\mathbf{r}) = \frac{1}{3} \left\{ \cos \left[2\pi \left[\sqrt{2/3}y + \frac{2}{\sqrt{3}}z + \frac{\phi}{2\pi} \right] \right] + 2 \cos \left[2\pi \left[\frac{1}{\sqrt{2}}x - \frac{1}{3} \right] \right] \cos \left[2\pi \left[\frac{-1}{\sqrt{6}}y + \frac{2}{\sqrt{3}}z + \frac{\phi}{2\pi} \right] \right] \right\},$$

$$w_2(\mathbf{r}) = \frac{1}{3} \left\{ \cos[2\pi(\sqrt{2}x - \frac{2}{3})] + 2 \cos \left[2\pi \left[\frac{1}{\sqrt{2}}x - \frac{1}{3} \right] \right] \cos[2\pi(\sqrt{3}/2y)] \right\}$$

(where x, y, z are in units of a , and ϕ is the azimuthal angle), and the functions η_0 , ξ_1 , and ξ_2 are now functions of $(x^2 + y^2)^{1/2} a |c_1''|^{-1/2}$. Hence our results for $\rho_D(\mathbf{r})$ quoted in Sec. I [cf. Eq. (1.5)].

Figures 5 and 6 show contour plots of $\rho(\mathbf{r})$, in the planes AB and CD , respectively [shown in Fig. 4; all these planes are perpendicular to the (111) plane, the plane of the paper]. Each figure shows the density contours for both the uniform bcc solid and the bcc solid with the $\frac{1}{2}a(1,1,1)$ screw dislocation.

These figures give a clear picture of the density distribution in the solid in the presence of the screw dislocation. We note the following features of our results.

(i) The density $\rho_D(\mathbf{r})$ in the presence of the dislocation retains the same periodicity in the z direction as in the uniform solid.

(ii) But the positions of the maxima of $\rho_D(\mathbf{r})$, however, are displaced along the z axis relative to that of $\rho(\mathbf{r})$ for the uniform solid, by amounts which are very close to those expected from continuum elasticity theory, namely $\mathbf{u} = \mathbf{b}\phi/2\pi$. So, if just these maxima were to be marked in Figs. 5 and 6, the results would be very similar to the conventional pictures of the dislocation (cf. Figs. 5(c) and 5(d) of Duesbery⁷).

(iii) However, the detailed density distribution in the core of the dislocation is very different from the conventional pictures. In particular, the modulation of $\rho_D(\mathbf{r})$ along the dislocation axis is small near the core. This can also be readily seen from Eq. (1.5) for $\rho_D(\mathbf{r})$. The z dependence of the density is only through the second term, and $\xi_1(r)$ vanishes at the core. Thus the dislocation core has a columnar character.

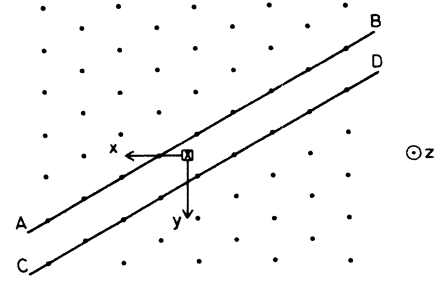


FIG. 4. The triangular lattice obtained by projection of the bcc lattice on to its (111) plane. The dislocation axis positioned at \square is perpendicular to this plane. AB and CD denote two planes parallel to the dislocation axis.

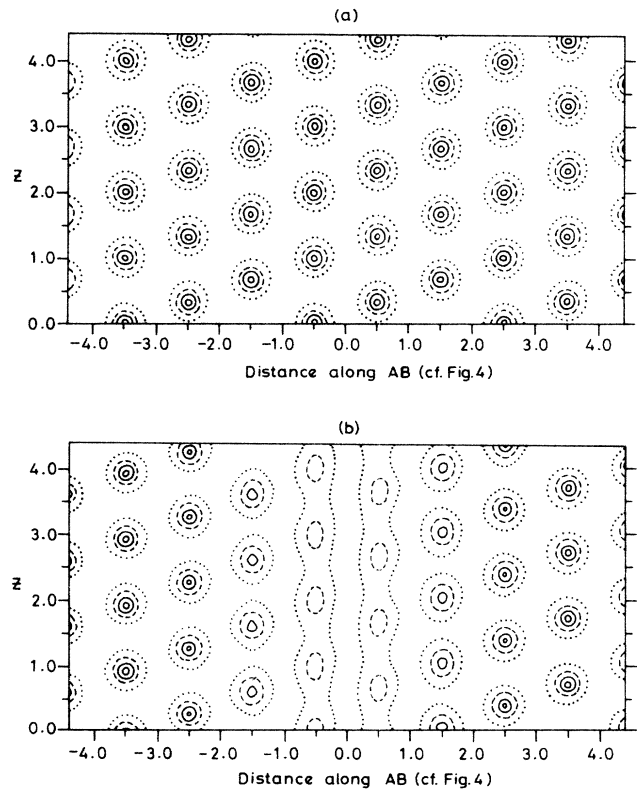


FIG. 5. Contours of constant density in the plane AB of Fig. 4: (a) for undistorted solid; (b) for solid with dislocation. The contour levels shown are for $\rho(r)/\rho_l = 1.0$ (dotted line), 7.4 (dashed line), 20.1 (outer solid line), and 33.1 (inner solid line). The horizontal and vertical distances are in units of $(\frac{2}{3})^{1/2}a$ and $(\sqrt{3}/2)a$, respectively, where a is the bcc lattice spacing.

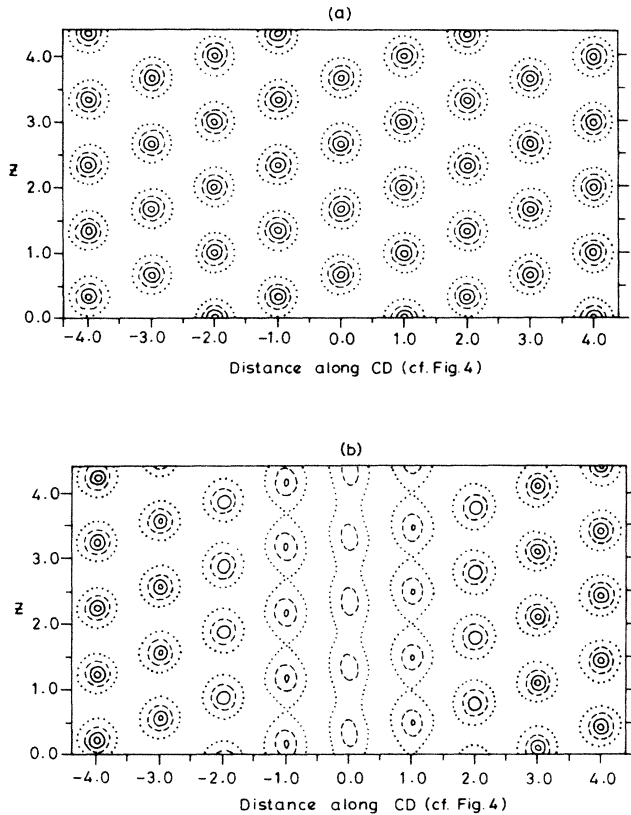


FIG. 6. Contours of constant density in the plane CD of Fig. 4: (a) for undistorted solid; (b) for solid with dislocation. The contour levels shown are for $\rho(r)/\rho_l = 1.0$ (dotted line), 7.4 (dashed line), 20.1 (outer solid line), and 33.1 (inner solid line). The horizontal and vertical distances are in units of $(\frac{2}{3})^{1/2}a$ and $(\sqrt{3}/2)a$, respectively, where a is the bcc lattice spacing.

VII. CONCLUDING DISCUSSION: THE PEIERLS-NABARRO BARRIER

There are two major improvements that need to be made to the calculations we have presented here.

The first is that we must perform calculations going beyond the gradient and local approximations used in this paper. This improvement is crucial for obtaining, within our formalism, the Peierls-Nabarro barrier. This barrier describes the dependence of the energy of the

dislocation on its location within the unit cell of the crystal, and has great influence on the mechanical properties of the crystal. It is easy to see that within the approximations presented in this paper, the energy of the dislocation is independent of its location; in other words the Peierls-Nabarro barrier is zero, and the dislocation can move freely through the crystal. This is, in one sense, a nice feature of our theory, for, experimentally inferred values for the Peierls-Nabarro barrier are actually very small²⁵ (10^{-6} of the extrapolated elastic energy needed for 10% strain, say). Now the degree of validity of the gradient and local approximation depends on the largeness of $|c_1''|$ (the larger the $|c_1''|$, the slower the spatial variation of the order parameters). Hence, in our theory the smallness of the Peierls-Nabarro barrier is understandable, and calculable perturbatively (by going beyond the gradient and local approximation) in terms of the small parameter $1/|c_1''|$. Such a calculation will be presented elsewhere.

The second improvement needed is that we must include much more of the detailed q dependence of the $c^{(2)}(q)$ than we have done here, where we kept only its first peak. This means including many more Fourier components of the molecular field than considered here. For the uniform crystal it is known that this has important effects on the energetics and relative stability of different crystal structures. Its effect on the energetics and structure of the dislocation must, hence, be studied. Of course this improvement renders the problem much harder computationally, and will probably necessitate the use of supercomputers.

We believe that given the above-mentioned improvements, the formalism presented here can be a viable and useful framework for investigating the structure and energetics of dislocation in crystals. Even more important, we hope to extend our formalism to calculate the structure and energetics of (large-angle) grain boundaries.

ACKNOWLEDGMENTS

We (T.V.R. and H.R.K.) thank the Department of Science and Technology, Government of India, and one of us (M.R.L.) thanks the Council for Scientific and Industrial Research, India for financial support. We also acknowledge useful conversations with C. Jayaprakash, and the use of The Ohio State University graphics facility during a visit to the Department of Physics there.

¹T. V. Ramakrishnan and M. Yussouff, *Phys. Rev. B* **19**, 2775 (1979).

²A. D. J. Haymet and D. W. Oxtoby, *J. Chem. Phys.* **74**, 2559 (1981).

³T. V. Ramakrishnan, *Pramana* **22**, 365 (1984).

⁴L. D. Landau and E. M. Lifshitz, *Theory of Elasticity* (Pergamon, New York, 1975); A. M. Kosevich, in *Dislocations in Solids*, edited by F. R. N. Nabarro (North-Holland, Amsterdam, 1979), Vol. 1; J. P. Hirth and J. Lothe, *Theory of Dislocations* (Wiley, New York, 1982).

⁵V. Vitek, R. C. Perrin, and D. K. Bowen, *Philos. Mag.* **21**, 1049 (1970).

⁶For some reviews, see M. P. Puls, in *Proceedings of the International Conference on Dislocation Modeling of Physical Systems* (Pergamon, Oxford, 1981), p. 249; J. W. Christian, *Metall. Trans. A* **14**, 123 (1983).

⁷M. S. Duesbery, *Comtemp. Phys.* **27**, 145 (1986).

⁸H. R. Krishnamurthy and T. V. Ramakrishnan (unpublished).

⁹D. W. Oxtoby and A. D. J. Haymet, *J. Chem. Phys.* **76**, 6262 (1982).

- ¹⁰A.D.J. Haymet, J. Chem. Phys. **78**, 4641 (1983); S. Smithline and A.D.J. Haymet, J. Chem. Phys. **83**, 4103 (1985).
- ¹¹A.D.J. Haymet and D.W. Oxtoby, J. Chem. Phys. **84**, 1769 (1986).
- ¹²C. Marshall, B. Laird, and A.D.J. Haymet, Chem. Phys. Lett. **122**, 320 (1985); see also, B. Bagchi, C. Cerjan, and S.A. Rice, J. Chem. Phys. **79**, 6222 (1983).
- ¹³A.D.J. Haymet, Phys. Rev. Lett. **52**, 1013 (1984); M. Rovere and M.P. Tosi, J. Phys. C **18**, 3445 (1985); see also B. Bagchi, C. Cerjan, U. Mohanty, and S. A. Rice, Phys. Rev. B **29**, 2857 (1984).
- ¹⁴G.L. Jones and U. Mohanty, Mol. Phys. **54**, 1241 (1985); P. Tarazona, Phys. Rev. A **31**, 2672 (1985); M. Baus and J.L. Colot, *ibid.* **55**, 653 (1985); J. Phys. C **18**, L365 (1985); J.L. Colot and M. Baus, Mol. Phys. **56**, 807 (1985); J. L. Colot, M. Baus, and H. Xu, *ibid.* **57**, 809 (1986).
- ¹⁵W.A. Curtin and N.W. Ashcroft, Phys. Rev. A **32**, 2909 (1985).
- ¹⁶W.A. Curtin and N.W. Ashcroft, Phys. Rev. Lett. **56**, 2775 (1986).
- ¹⁷J.L. Barrat (private communication).
- ¹⁸P. Tarazona, Mol. Phys. **52**, 81 (1984).
- ¹⁹J. L. Barrat, M. Baus, and J. P. Hansen, Phys. Rev. Lett. **56**, 1063 (1986), (unpublished); S. J. Smithline and A.D.J. Haymet (unpublished).
- ²⁰N. H. March and M. P. Tosi, Phys. Chem. Liq. **10**, 185 (1980); **11**, 79 129 (1981); M. Rovere, M. P. Tosi, and N. H. March, *ibid.*, **12**, 177 (1982); B. D'Aguzzo, M. Rovere, M. P. Tosi, and N. H. March, *ibid.* **13**, 113 (1983); M. Rovere and M. P. Tosi, Solid State Commun. **55**, 1109 (1985); H. E. Roman and W. Dieterich (unpublished).
- ²¹A. D. J. Haymet (unpublished).
- ²²P. Harrowell and D. W. Oxtoby, J. Chem. Phys. **80**, 1639 (1984).
- ²³A.L. Fetter and P.C. Hohenberg, in *Superconductivity*, edited by R.D. Parks (Dekker, New York, 1969), Vol. II.
- ²⁴This is because the coefficients μ_{12} and μ_{111} evaluated at $\xi_1=0$, $\xi_2=b_2$ are zero.
- ²⁵See, for example, M. P. Puls, in *Proceedings of the International Conference on Dislocation Modelling of Physical Systems*, Ref. 6, p. 258.